

## Cascade Reactions

# Photochemical Approach to the Cyclohepta[*b*]indole Scaffold by Annulative Two-Carbon Ring-Expansion

Dina Christina Tymann, Lars Benedix, Lyuba Iovkova, Roman Pallach, Sebastian Henke, David Tymann, and Martin Hiersemann<sup>\*[a]</sup>

**Abstract:** We report on the implementation of the concept of a photochemically elicited two-carbon homologation of a  $\pi$ -donor– $\pi$ -acceptor substituted chromophore by triple-bond insertion. Implementing a phenyl connector between the slide-in module and the chromophore enabled the synthesis of cyclohepta[*b*]indole-type building blocks by a metal-free annulative one-pot two-carbon ring expansion of the five-membered chromophore. Post-irradiative structural elaboration provided founding members of the indolo[2,3-*d*]tropone family of compounds. Control experiments in combination with computational chemistry on this multibond reorganization process founded the basis for a mechanistic hypothesis.

The *N*-heteroacene cyclohepta[*b*]indol<sup>[1]</sup> (**1**) features the basic scaffold of a variety of man-made pharmaceutically active compounds<sup>[2]</sup> and natural products,<sup>[3]</sup> for example, alstonlarsine A (**2**)<sup>[4]</sup> (Figure 1). To address the challenges associated with the synthesis of cyclohepta[*b*]indol-type building blocks, a well-diversified portfolio of enabling synthetic methods is already available.<sup>[5]</sup> Variations of annulation reactions,<sup>[6]</sup> of (*m*+*n*)-cycloadditions,<sup>[7]</sup> and of the Cope rearrangement<sup>[8]</sup> have proven particularly valuable. Notably, however, organic photochemistry has not yet been exploited to access perhydrocyclohepta[*b*]indole-type building blocks (**3**).

To complement the existing methodology, we aimed for a *fuse–compress–expand* sequence to 6,7-dihydro-cyclohepta[*b*]indol-8(*5H*)-ones **4** that exploits an unprecedented photochemically triggered two-carbon ring-expansion (Figure 2).<sup>[9]</sup> *Fusing* is accomplished by Sonogashira cross-coupling between *o*-iodo anilines (**5**) and terminal alkynes (**6**), followed by condensation with five-membered cyclic 1,3-dicarbonyl com-

pounds (**7**) and finalized by *N*-acylation to deliver photochemistry-competent vinylogous amides **8**. The subsequent *compress-and-expand* phase consists of a photochemically triggered formation of a transient [2+2]-cycloadduct that subsequently collapses to deliver the 6,7-dihydro-cyclohepta[*b*]indol-8(*5H*)-one **4**; hence, the actual ring-expansion merges excited-state with ground state chemistry to an unprecedented one-pot process.

The experimental procedures and characterization data for the products **8** of the *fuse*-phase are provided in full detail in the Supporting Information (29 examples). The results of our study on the photochemically triggered two-carbon ring-expansion of **8** are summarized in Tables 1–3. We adopted our previously optimized conditions for the alkyne de Mayo reaction without the necessity of optimization. Hence, solutions of the *N*-protected vinylogous amides **8a–ab** (0.16 mmol) in degassed 2,2,2-trifluoroethanol (TFE, *c* = 0.03 M) were irradiated in sealable quartz tubes using the low-pressure mercury vapor lamps ( $E_{\text{max}}$  = 254 nm) of a commercially available photoreactor. Reaction times refer to reactor running times. The appearance

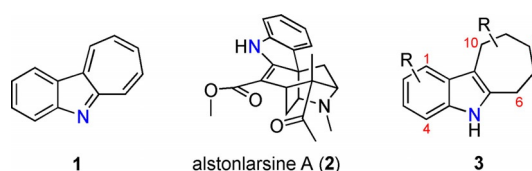


Figure 1. Motif (1), Variation (2), and Building Block (3).

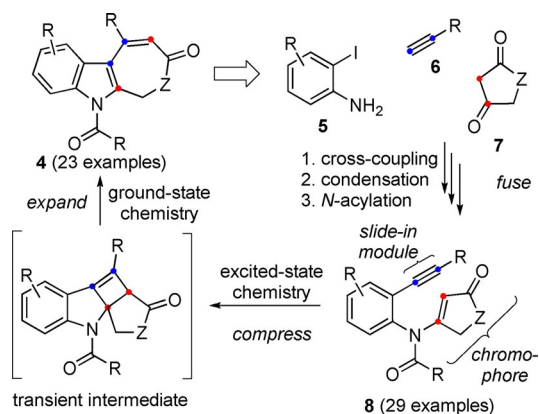


Figure 2. *Fuse–compress–expand* strategy to 6,7-dihydrocyclohepta[*b*]indol-8(*5H*)-ones.

[a] Dr. D. C. Tymann, L. Benedix, Dr. L. Iovkova, R. Pallach, Prof. Dr. S. Henke, Dr. D. Tymann, Prof. Dr. M. Hiersemann  
Fakultät für Chemie und Chemische Biologie  
TU Dortmund, 44227 Dortmund (Germany)  
E-mail: martin.hiersemann@tu-dortmund.de

Supporting information and the ORCID identification number(s) for the author(s) of this article can be found under:  
<https://doi.org/10.1002/chem.202002581>.

© 2020 The Authors. Published by Wiley-VCH GmbH. This is an open access article under the terms of Creative Commons Attribution NonCommercial-NoDerivs License, which permits use and distribution in any medium, provided the original work is properly cited, the use is non-commercial and no modifications or adaptations are made.

of yellow colored reaction mixtures served as an indicator for product formation and progression of conversion was detected by TLC analysis.

Representative examples for aliphatic and aromatic substituents at C-10 were initially screened (Table 1). Ring expansion proceeded for  $R^1 = \text{octyl-}$  (**8a**), 4-hydroxybutyl- (**8b**) and 4-siloxybutyl (**8c**) to deliver **4a–c** in useful yields (85–92%). Somewhat unexpectedly, hydroxymethyl-substitution (**8d**) triggered decomposition under irradiation. No defined degradation product could be isolated. The nature of the decomposition pathway(s) remains speculative. Fortunately, irradiation of the corresponding silyl ether **8e** delivered the ring-expansion product **4e** in 86% yield. 2-Aminotolane-derived **8f** was susceptible to ring-expansion at prolonged reaction times and delivered the  $R^1 = \text{phenyl}$  substituted **4f** in moderate yield (52%).

For pharmaceutically relevant cyclohepta[b]indoloids, substituent diversification at C-2 is frequently found.<sup>[2]</sup> Consequently, we moved on to study substituent effects for  $R^2 \neq \text{H}$  at C-2 and using  $R^1 = \text{CH}_3$  at C-10 as a prototype for alkyl substitution (Table 2). Methyl- (**8g**), trifluoromethyl- (**8h**) and *tert*-butyl-substitution (**8i**) at C-2 were tolerated and **4g–i** were isolated in valuable yields (75–91%). 4-Aminobiphenyl-based **8j** underwent the ring-expansion slowly and sluggishly to provide **4j** (26%) in low yield. Bromo or fluoro substitution enabled access to **4k** (83%) or **4l** (83%). Suzuki–Miyaura cross-coupling of **4k** with phenylboronic acid under carefully optimized conditions delivered **4j** (92%); thus **4k** may serve as a relay compound for post-ring expansion structural diversification (vide infra).<sup>[10]</sup>  $\pi$ -Donor ( $R^2 = \text{OCH}_3$ ) and  $\pi$ -acceptor ( $R^2 = \text{CO}_2\text{Me}$  or CN) substitution allowed the formation of **4m** (57%), **4n** (86%), and **4o** (86%). However, no conversion was observed for  $R^2 = \text{NO}_2$  (**8p**, not depicted).

We proceeded to study substituent effects at C-3 or C-4 for  $R^2 = \text{H}$  at C-2 and  $R^1 = \text{CH}_3$  at C-10. (Table 3). Subjecting vinylogous amides featuring methyl (**8q**), fluoro (**8r**), or chloro (**8s**) substitution at C-3 to the ring-expansion protocol afforded **4q** (90%), **4r** (83%), and **4s** (86%) in valuable yields. Ring-expansion

**Table 1.** Two-carbon ring expansion: Varying  $R^1$ .

Starting Material	Product	Time (h)	Yield (%)
<b>8a</b> ( $R^1 = \text{CH}_3(\text{CH}_2)_7$ )	<b>4a</b>	4.5	91%
<b>8b</b> ( $R^1 = \text{HOCH}_2(\text{CH}_2)_3$ )	<b>4b</b>	4.5	85%
<b>8c</b> ( $R^1 = \text{TBSOCH}_2(\text{CH}_2)_3$ )	<b>4c</b>	4.75	92%
<b>8d</b> ( $R^1 = \text{HOCH}_2$ )	(decomp.)	-	-
<b>8e</b> ( $R^1 = \text{TBSOCH}_2$ )	<b>4e</b>	5.25	86%
<b>8f</b> ( $R^1 = \text{Ph}$ )	<b>4f</b>	72	52%

**Table 2.** Two-carbon ring expansion: Varying  $R^2$ .

Starting Material	Product	Time (h)	Yield (%)
<b>8g</b> ( $R^2 = \text{H}$ )	<b>4g</b>	4	75%
<b>8h</b> ( $R^2 = \text{F}_3\text{C}$ )	<b>4h</b>	5	84%
<b>8i</b> ( $R^2 = \text{t-Bu}$ )	<b>4i</b>	5	91%
<b>8j</b> ( $R^2 = \text{Ph}$ )	<b>4j</b>	36	26%
<b>8k</b> ( $R^2 = \text{Br}$ )	<b>4k</b>	5.75	83%
<b>8l</b> ( $R^2 = \text{F}$ )	<b>4l</b>	4.5	83%
<b>8m</b> ( $R^2 = \text{MeO}$ )	<b>4m</b>	5.5	57%
<b>8n</b> ( $R^2 = \text{NC}$ )	<b>4n</b>	7.5	86%
<b>8o</b> ( $R^2 = \text{CO}_2\text{Me}$ )	<b>4o</b>	7.25	86%

[a] PhB(OH)<sub>2</sub> (1.5 equiv), Pd(PPh<sub>3</sub>)<sub>2</sub>Cl<sub>2</sub> (0.05 equiv), PCy<sub>3</sub> (0.1 equiv), Cs<sub>2</sub>CO<sub>3</sub> (1.5 equiv), 1,4-dioxane (297 equiv), 80 °C, 5.5 h, 92% (226 mg).

**Table 3.** Two-carbon ring expansion: Varying  $R^{1-4}$  and Z.

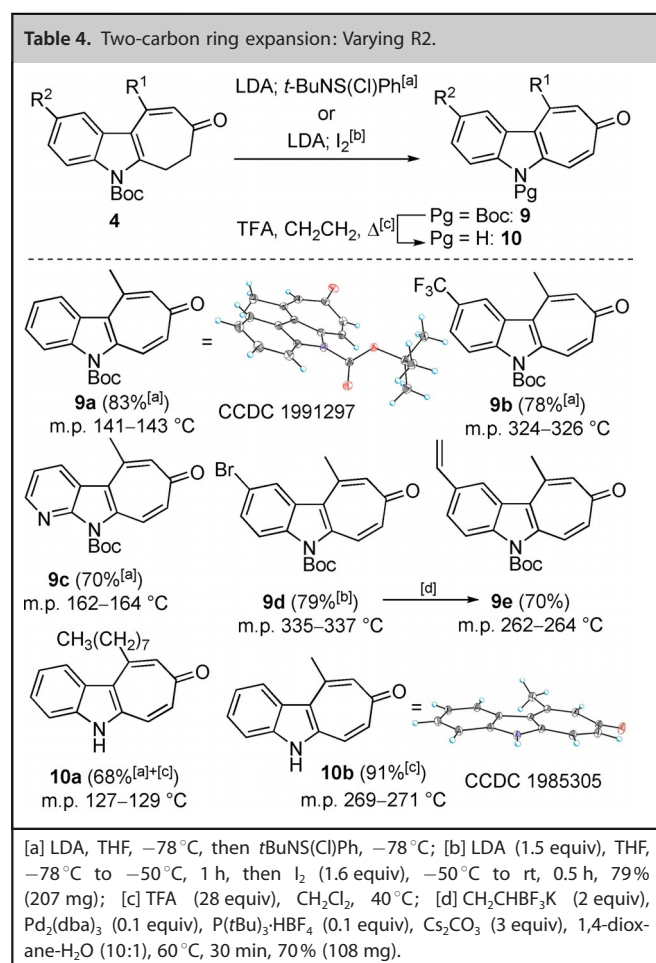
Starting Material	Product	Time (h)	Yield (%)
<b>8q</b> ( $R^1 = \text{CH}_3$ )	<b>4q</b>	4	90%
<b>8r</b> ( $R^1 = \text{CH}_3$ , $R^2 = \text{F}$ )	<b>4r</b>	4.5	83%
<b>8s</b> ( $R^1 = \text{CH}_3$ , $R^2 = \text{Cl}$ )	<b>4s</b>	6.5	86%
<b>8t</b> ( $R^1 = \text{CH}_3$ , $R^2 = \text{MeO}$ )	<b>4t</b>	60	66%
<b>8u</b> ( $R^1 = \text{CH}_3$ , $R^2 = \text{Ph}$ )	(decomp.)	-	-
<b>8v</b> ( $R^1 = \text{CH}_3$ , $R^2 = \text{Ph}$ )	(96 h, no conv.)	-	-
<b>8w</b> ( $R^1 = \text{CH}_3$ , $R^2 = \text{Ph}$ )	<b>4y</b>	2.75	86%
<b>8x</b> ( $R^1 = \text{CH}_3$ , $R^2 = \text{Ph}$ )	<b>4x</b>	35	52%
<b>8z</b> ( $R^1 = \text{CH}_3$ , $R^2 = \text{Me}_3\text{Si}$ )	(3 h, no conv.)	-	-
<b>8aa</b> ( $R^1 = \text{CH}_3$ , $R^2 = \text{Me}_3\text{Si}$ )	<b>4aa</b>	6	51%
<b>8ab</b> ( $R^1 = \text{CH}_3$ , $R^2 = \text{Me}_3\text{Si}$ )	<b>4ab</b>	60	41%

sion of *m*-aminobenzoic acid derived **8t** ( $R^1 = \text{CH}_3$ ,  $R^3 = \text{CO}_2\text{Me}$ ) required strikingly prolonged irradiation (60 h, **4o**: 7 h) and delivered **4t** (66%, **4o**: 86%) in moderate yield. Degradation was observed for  $R^4 = \text{CH}_3$  (**8u**); in the event, we speculate that „steric hindrance“ interferes with the photochemical compress-phase of the ring-expansion process. 2-Aminonaphthalene-based **8w** resisted irradiation (96 h) and was re-isolated (96%), whereas irradiation of the 5,6,7,8-tetrahydro-2-aminonaphthalene-based **8v** proceeded reluctantly to afford tetracyclic **4v** (50%) in moderate yield. 5-Aminobenzo[*d*][1,3]dioxole-derived **8x** successfully underwent the ring-expansion to yield tetracyclic **4x** (52%) in reasonable yield. Finally, we turned to chromophore diversification. Irradiation of *N*-acetyl derivative **8y** yielded the ring-expanded product **4y** in 86% yield after only 2.75 h of reactor running time. When irradiating tetrone acid-originated **8z** ( $R^1 = \text{CH}_3$ ,  $Z = \text{O}$ ), no conversion was detected by TLC. Tetramic acid-derived **8aa** ( $R^1 = \text{CH}_3$ ) and **8ab** ( $R^1 = \text{Si}(\text{CH}_3)_3$ ), however, could be converted into the desired ring-expansion products **4aa** (51%) and **4ab** (41%) with moderate success.

We are interested in utilizing indole-tropone-fused cyclohepta[*b*]indol-8-ones (indolo[2,3-*d*]tropones, **10**) as scaffold elements for the synthesis of extended *N*-heteroacenes, *N*-heterohelicenes, and as building blocks in natural product total synthesis (Table 4). Thus, we explored the dehydrogenation of se-

lected 6,7-dihydro-cyclohepta[*b*]indol-8(5*H*)-ones **4**. The corresponding lithium enolates were treated with *N*-*tert*-butylbenzenesulfinimidoyl chloride<sup>[11]</sup> to deliver Boc-protected indolo[2,3-*d*]tropones **9**.<sup>[12,13]</sup> Purification of the thus prepared cyclohepta[*b*]indol-8-ones **9** was complicated by intractable impurities of *N*-(*tert*-butyl)-5-phenylthiohydroxylamine. Alternatively, the enolate of **4k** was treated with  $\text{I}_2$  to deliver Boc protected **9d** (79%); aryl bromide **9d** is anticipated to serve as a relay compound for scaffold extension as exemplified by Suzuki cross-coupling with potassium vinyltrifluoroborate to afford **9e** (70%). Removal of the Boc protecting group delivered **10a** (68%) and **10b**<sup>[12]</sup> (91%) representing founding members of the indolo[2,3-*d*]tropone (**10**) family of compounds.<sup>[14,15,16]</sup>

We used experimental and computational studies to gain mechanistic insights into the ring-expansive multibond reorganization process. Experimentally, irradiation (350 nm) of **8k** in the presence of a triplet sensitizer (xanthone) triggered formation of **4k**; on the other hand, formation of **4k** was suppressed at 254 nm in the presence of a triplet quencher (2,5-dimethylhexa-2,4-diene).<sup>[17]</sup> On this basis, we assumed a [2+2] cycloaddition on the triplet surface. To gain further mechanistic insights, we performed (TD)DFT studies using the model compound **11** (Figure 3).<sup>[18,19]</sup> Our calculations on the B3LYP/def2-TZVP level of theory predict a vertical excitation of  $S_0$ -**11** to an upper  $S_n$ -state (+112.6 kcal mol<sup>-1</sup>) that is followed by internal conversion (IC) to the  $S_1$ -**11** state ( $n, \pi^*$  character with respect to the  $\alpha, \beta$ -enone segment) and intersystem crossing (ISC) to the  $T_1$ -**11** state.<sup>[20]</sup> Our computations suggest  $\pi, \pi^*$  character for  $T_1$ -**11** with spin-density being located above and below the  $\alpha, \beta$ -enone segment. Subsequent low-barrier (+4.8 kcal mol<sup>-1</sup>) 5-*exo*-dig cyclization to  $T_1$ -**13** via **12** is predicted to be highly exoenergetic (-21.1 kcal mol<sup>-1</sup>).  $T_1$ -**13** was calculated to be almost isoenergetic to the double bond isomeric  $T_1$ -**14** (-0.5 kcal mol<sup>-1</sup>);  $T_1$ -**13** is interconnected with  $T_1$ -**14** via a low-barrier transition state (+1.8 kcal mol<sup>-1</sup>, not depicted). Rapid ISC of  $T_1$ -**14** to  $S_0$ -**14** is followed by an almost barrier-less (+1.1 kcal mol<sup>-1</sup>) and highly exoenergetic (-42.1 kcal mol<sup>-1</sup>) cyclization via **15** to the (2+2) photocycloadduct **16**. According to gas-phase DFT calculations, the  $\pi$ -donor- $\pi$ -acceptor substituted cyclobutene segment of **16** is susceptible to a slightly endoenergetic (+2.8 kcal mol<sup>-1</sup>) concerted bond reorganization via the transition-state **17** (+24.1 kcal mol<sup>-1</sup>) to afford **18** featuring a *trans*- $\alpha, \beta$ -enone moiety.<sup>[21]</sup> The stereochemical result of the modeled conversion of **16** to **18** is in accordance with a bond reorganization proceeding by a conrotatory 4 $\pi$ -electrocyclic ring-opening. Although predicted to be highly exoenergetic, attempts to localize a pathway leading from **18** (or **16**) to the model compound **19** for the experimentally observed ring expansion-products by gas-phase computations were futile. The scale of the predicted barrier height (+24.1 kcal) for the conversion of **16** to **18** encouraged experimental studies to identify the [2+2]-cycloadduct. However, efforts to detect the elusive [2+2]-cycloadduct from **8k** by (preparative) TLC or by NMR experiments in deuterated solvents failed. The ring-opening was then re-modeled by considering explicit hydrogen-bonding interactions between two molecules of 2,2,2-trifluor-







- [6] For selected recent examples, see: a) J. Kaufmann, E. Jäckel, E. Haak, *Angew. Chem. Int. Ed.* **2018**, *57*, 5908–5911; *Angew. Chem.* **2018**, *130*, 6010–6014; b) M. A. Kroc, A. Prajapati, D. J. Wink, L. L. Anderson, *J. Org. Chem.* **2018**, *83*, 1085–1094; c) A. S. Jadhav, Y. A. Pankhade, R. Vijaya Anand, *J. Org. Chem.* **2018**, *83*, 8615–8626; d) Q. Zeng, K. Dong, J. Huang, L. Qiu, X. Xu, *Org. Biomol. Chem.* **2019**, *17*, 2326–2330; e) L. Zhang, Y. Zhang, W. Li, X. Qi, *Angew. Chem. Int. Ed.* **2019**, *58*, 4988–4991; *Angew. Chem.* **2019**, *131*, 5042–5045.
- [7] For selected recent examples, see: a) T. Takeda, S. Harada, A. Okabe, A. Nishida, *J. Org. Chem.* **2018**, *83*, 11541–11551; b) C. Gelis, G. Levitre, J. Merad, P. Retailleau, L. Neuville, G. Masson, *Angew. Chem. Int. Ed.* **2018**, *57*, 12121–12125; *Angew. Chem.* **2018**, *130*, 12297–12301; c) Z. Wang, Y. Addepalli, Y. He, *Org. Lett.* **2018**, *20*, 644–647; d) A. N. Parker, M. C. Martin, R. Shenje, S. France, *Org. Lett.* **2019**, *21*, 7268–7273; e) J. Xu, V. H. Rawal, *J. Am. Chem. Soc.* **2019**, *141*, 4820–4823.
- [8] For selected recent examples, see: a) G. Xu, L. Chen, J. Sun, *Org. Lett.* **2018**, *20*, 3408–3412; b) M. Häfner, Y. M. Sokolenko, P. Gamedinger, E. Stempel, T. Gaich, *Org. Lett.* **2019**, *21*, 7370–7374.
- [9] For the initial example, see: D. Tymann, D. C. Tymann, U. Bednarzick, L. Iovkova-Berends, J. Rehbein, M. Hiersemann, *Angew. Chem. Int. Ed.* **2018**, *57*, 15553–15557; *Angew. Chem.* **2018**, *130*, 15779–15783.
- [10] Conditions adapted from: E. N. Agbo, T. J. Makhafola, Y. S. Choong, J. M. Mphatele, P. Ramasami, *Molecules* **2015**, *21*, 28.
- [11] T. Mukaiyama, J.-i. Matsuo, H. Kitagawa, *Chem. Lett.* **2000**, *29*, 1250–1251.
- [12] Deposition numbers 1991297 and 1985305 (**9a** and **10b**) contain the supplementary crystallographic data for this paper. These data are provided free of charge by the joint Cambridge Crystallographic Data Centre and Fachinformationszentrum Karlsruhe Access Structures service.
- [13] Structural assignment in solid state and in solution is in accordance with the notion of **9** as cyclohepta[b]indol-8(5H)-one and not as tautomeric cyclohepta[b]indol-8-ol.
- [14] To the best of our knowledge, parent indolo[2,3-*d*]troponone has been mentioned only once, see: T. Nozoe, H. Horino, T. Toda, *Tetrahedron Lett.* **1967**, *8*, 5349–5353.
- [15] For the synthesis of indolo[2,3-*b*]tropones, see: a) K. Yamane, K. Fujimori, *Bull. Chem. Soc. Jpn.* **1976**, *49*, 1101–1104; b) J. Jiye, I. Kunihiro, T. Fumiki, O. Mitsunori, *Chem. Lett.* **2010**, *39*, 861–863; c) J. De Jong, J. H. Boyer, *J. Org. Chem.* **1972**, *37*, 3571–3577.
- [16] For the synthesis of indolo[3,2-*b*]tropones, see: a) U. K. Mishra, S. Yadav, S. S. V. Ramasastry, *J. Org. Chem.* **2017**, *82*, 6729–6737; b) see also reference 15a).
- [17] For experimental details, see the Supporting Information.
- [18] For computational details, see the Supporting Information.
- [19] For related computational studies, see: a) E. García-Expósito, M. J. Bearpark, R. M. Ortuño, M. A. Robb, V. Branchadell, *J. Org. Chem.* **2002**, *67*, 6070–6077; b) J. R. Cucarull-González, J. Hernando, R. Alibés, M. Figueredo, J. Font, L. Rodríguez-Santiago, M. Sodupe, *J. Org. Chem.* **2010**, *75*, 4392–4401.
- [20] O. Schalk, M. S. Schuurman, G. Wu, P. Lang, M. Mucke, R. Feifel, A. Stolow, *J. Phys. Chem. A* **2014**, *118*, 2279–2287.
- [21] For mechanistic studies concerning the electrocyclic ring opening of fused cyclobutenes, see: a) C. Silva López, O. N. Faza, Á. R. de Lera, *Chem. Eur. J.* **2007**, *13*, 5009–5017; b) X.-N. Wang, E. H. Krenske, R. C. Johnston, K. N. Houk, R. P. Hsung, *J. Am. Chem. Soc.* **2014**, *136*, 9802–9805; c) M. J. Ralph, D. C. Harrowven, S. Gaulier, S. Ng, K. I. Booker-Milburn, *Angew. Chem. Int. Ed.* **2015**, *54*, 1527–1531; *Angew. Chem.* **2015**, *127*, 1547–1551.
- [22] For *N*-Boc cleavage in fluorinated alcohols at elevated temperatures, see: J. Choy, S. Jaime-Figueroa, L. Jiang, P. Wagner, *Synth. Commun.* **2008**, *38*, 3840–3853.

Manuscript received: May 27, 2020

Accepted manuscript online: May 28, 2020

Version of record online: August 17, 2020